

Effect of wind and buoyancy on hydrogen release and
dispersion in a compartment with vents at multiple
levels

Kuldeep Prasad, William Pitts, Jiann Yang
National Institute of Standards and Technology
Gaithersburg, MD 20899

March 2, 2010

Prepared for publication in
International Journal of Hydrogen Energy

Corresponding Author:

Kuldeep Prasad

e-mail: kuldeep.prasad@nist.gov

Phone : 301-975-3968

Effect of Wind and Buoyancy on Hydrogen Release and Dispersion in a Compartment with Vents at Multiple Levels

Abstract

The natural and forced mixing and dispersion of hydrogen released in an accidental manner in a partially enclosed compartment with vents at multiple heights is investigated using theoretical tools. The key to the analysis is determination of the position of neutral buoyancy plane, where the pressure in the compartment is equal to that of the exterior. Air flows in through vents below the position of neutral buoyancy and exits from vents above it. CFD simulations are conducted to confirm the physical phenomena and to compare with the analytical results. The analytical model is useful in understanding the important physical processes involved during hydrogen release and dispersion in a compartment with vents at multiple levels, with and without a steady wind. Parametric studies are conducted to identify the relative importance of various parameters. Model results indicate that the steady state hydrogen volume fraction in the compartment is lower when the hydrogen release rate is smaller and the vent cross-sectional area is larger. Results also indicate that the fastest way to reduce flammable levels of hydrogen concentration in a compartment can be accomplished by blowing on the vents.

1 INTRODUCTION

Development of the hydrogen economy will require a better understanding of the potential for fires and explosions associated with the unintended release of hydrogen within a structure. The physical and chemical properties of hydrogen are sufficiently different from hydrocarbon fuels, and as a result the dispersion, mixing and burning behavior of hydrogen is also very different from that of conventional fuels [1]. Predicting the temporally and spatially evolving hydrogen concentration in a compartment with leaks whose size and location may be unknown is a challenging task. The uncertainty in predicting the concentrations can increase due to external forces such as wind and thermal gradients. Developing a methodology for accurately predicting the dispersion and mixing of hydrogen, when released accidentally from a fuel cell in a compartment or a vehicle parked in a residential garage is critical to the safe use of hydrogen and for the development of appropriate safety codes and standards for hydrogen applications.

The dispersion, mixing and combustion of hydrogen has been studied extensively and reported in various articles presented during the International Conferences on Hydrogen Safety [2], [3]. Swain et al. [4], [5] have developed a method to establish the requirements for venting in buildings that contain hydrogen fueled equipment, using a four step process. In the first step of their proposed methodology, the accident scenario should be constructed with helium released at the expected hydrogen leakage rate. Helium concentrations versus time should be measured at various locations. Secondly, Computational Fluid Dynamics (CFD) simulations should be performed of the accident scenario (using helium) and the model should be validated with experimental data. Thirdly, the CFD model should be used to predict the behavior of hydrogen (instead of helium) and finally, the risk from the spatial and temporal distribution of hydrogen can be determined. Experiments and numerical simulations [5] were performed in various geometric configurations to show that the methodology was suitable for assessing the risk from an accident scenario.

CFD software has been used extensively in the past to study hydrogen leakage and burning in complex geometries [6]-[9]. Swain and Shriber [6] have compared FLUENT (a commercial CFD software) calculations for a gas cloud formation for four different fuels

including hydrogen following an accidental scenario. In a separate study, as part of the HYSAFE program [7], an intercomparison exercise was performed with 10 different CFD codes using different turbulence models to simulate the vertical release of 1 g/s of hydrogen into a rectangular room with two small openings in the front wall. The NIST Fire Dynamics Simulator (FDS) has been used to simulate a set of reduced scale experiments where helium was used as a surrogate gas [8], [9]. These calculations have indicated that CFD software is capable of simulating the release and mixing of hydrogen with clearly defined geometries and boundary conditions, but simple analytical models are needed for development of appropriate codes and standard applications for hydrogen safety.

Analytical approaches have also been employed for studying the release of buoyant gases in a partially enclosed compartment [10]-[17]. These studies have typically focused on studying the effect of upper and lower openings in a room. Theoretical models have been developed for ventilation flows in a room with a heated floor [10], [11], [12], [15], however, these models typically look at the effect of point heating or distributed heating of the entire floor instead of the release of a buoyant gas. Zhang et. al [16] have modified the analytical models originally developed for smoke filling inside a compartment for the case of a hydrogen plume in a compartment. This model did not consider the effect of multiple vents nor did they allow for the effect of an external wind / thermal effects that have been considered in the current paper. Barley et. al [17] have developed a simple one-dimensional model for understanding the hydrogen stratification in a compartment that is ventilated through two leaks. Their model was limited to identifying the steady-state condition and did not consider the effect of multiple vents and an external wind flow. The results described in this paper are more general as they cover the transient as well as the steady-state flows that develop in a partially enclosed compartment.

A number of papers [18], [19], [20] have reported experimental data on release and dispersion of hydrogen or helium [2], [3]. Pitts et. al [21] have presented a detailed experimental study on helium dispersion in a $\frac{1}{4}$ -scale two-car residential garage. Time resolved measurements at multiple locations in the compartment were performed, and results were presented as a function of gas flow rates and duration of the flow. The experimental data presented in [21] has been compared with numerical simulations as reported in [8], [9]. The experimental

data has clearly been very useful in validating the numerical models and for improving our understanding of the physical processes.

A standard full tank of hydrogen in a typical hydrogen fueled vehicle contains approximately 5 kg of hydrogen. The rate at which hydrogen can leak from the tank is highly dependent on the instantaneous pressure in the tank and the size and location of the cracks in the tank or construction of the pressure release valve. When hydrogen is released accidentally in a compartment, the turbulent hydrogen plume that develops above the release point entrains ambient fluid as it rises. Once the plume reaches the top, it spreads radially outwards to form a buoyant layer separated from the ambient layer below by a density interface. As the depth of this buoyant layer increases, the interface descends towards the plume source, and the layer is fed with increasing buoyant fluid. The flow field can be significantly different if an obstruction is placed in the path of the hydrogen plume, for example, hydrogen release under a vehicle or leakage from a fuel cell placed under a shelf. Under such a scenario, the buoyant gas mixes rapidly with the surrounding air due to the presence of the obstruction. The turbulent mixing of hydrogen with air under an obstruction and its break up and release in the form of multiple independent plumes from multiple locations, results in a well mixed hydrogen air mixture in the compartment. As more hydrogen is released, the density of the compartment gradually reduces, and a ventilation regime develops in which cold air enters through the lower vent and warm air exits through the upper vent.

In this paper we develop simple analytical models for studying hydrogen release and dispersion in a compartment where the rising hydrogen plume is disrupted by the presence of an obstruction. The analysis involves the determination of the height of neutral buoyancy in a well mixed compartment. We use this concept to understand the impact of introducing vents at intermediate heights and calculate the resulting flows. This approach can be used to calculate the new height of the neutral buoyancy, and hence the process can be repeated to assess the impact of introducing further intermediate level vents. CFD simulations are conducted to confirm the physical phenomena and to compare with the analytical model. The effect of hydrogen release rate, vent location, vent cross-sectional area and thermal gradients on hydrogen volume fraction and location of the neutral layer in the compartment is discussed. The role of a steady wind that assists the buoyancy driven flow is then assessed.

Finally, simple models are presented for estimating the time that it takes for hydrogen to vent out of the garage, once the hydrogen release rate has been discontinued.

2 Hydrogen Release and Mixing in a Partially Enclosed Compartment

Consider the case of a partially enclosed compartment of height H , in which hydrogen is leaked accidentally under an obstruction (e.g. hydrogen release under a vehicle or release of hydrogen from a fuel cell placed under an obstruction). Turbulent mixing of the buoyant hydrogen gas with air under the obstruction, results in a well stirred mixture of hydrogen and air in the compartment. The compartment is assumed to be ventilated through two vents; “Vent 1” is located at the base of the compartment close to the floor and is also referred to as the “lower” vent, while “Vent 3” is located at the top of the compartment, also referred to as the “upper” vent. The two vents have cross-sectional area a_1 and a_3 , respectively. Here the suffixes 1 and 3 correspond to the respective vents. Note that subscript 2 will be used to denote intermediate level vents, discussed later in section 2.3. Figure 1 shows a schematic diagram of the compartment of height H , and with vents located close to the floor and close to the ceiling.

Let \dot{M}_{H_2} be the mass flow rate of pure hydrogen gas leaked accidentally into the compartment. As the flow from the source commences, there will be an outflow from both the upper and lower vents. This is due to a slight pressure increase in response to the sudden introduction of hydrogen into the compartment. As some of the gases are allowed to escape from the enclosure, this pressure rise becomes negligibly small. As the hydrogen gas mixes with the air in the compartment, the density structure within the compartment evolves. We assume that the air within the compartment is well mixed and that the concentration of hydrogen is uniform everywhere. The pressure within and outside the compartment varies hydrostatically with depth. Owing to the lower density of gas mixture inside the compartment, the vertical pressure gradient is lower than the vertical pressure gradient outside the compartment. These gradients are primarily due to the weight of the fluid. The difference

between these pressure gradients leads to a buoyancy driven flow through the vents [10], [12].

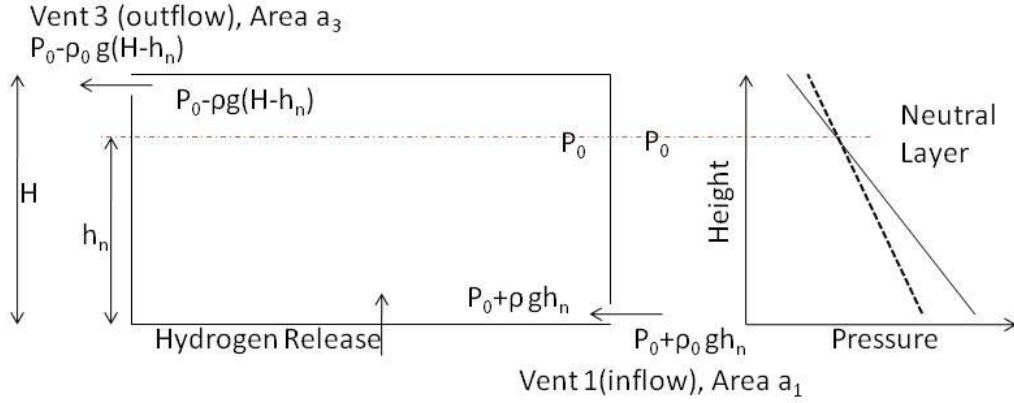


Figure 1: Schematic diagram of a compartment with vents at the top and bottom showing the location of the neutral layer. The variation of pressure as a function of height within the compartment (dashed line) and outside of the compartment (solid line) are also indicated.

We denote the velocity of the fluid through the lower and upper vent as v_1 and v_3 , respectively. In general, the velocity v_j of a gas mixture through a vent j is related to the pressure drop ΔP_j using the Bernoulli's theorem,

$$v_j = \sqrt{\frac{2\Delta P_j}{\rho}}, \quad (1)$$

where, ρ corresponds to the density of the gas mixture. The volumetric flow rate Q_j through vent j of area a_j is then related to the velocity v_j according to

$$Q_j = a_j v_j c_j, \quad (2)$$

where c_j is the discharge coefficient that accounts for the reduction in the area of the streamlines through the vent. The discharge coefficient is a constant lying between 0.5 for a sharp expansion at the inlet and 1.0 for a perfectly smooth expansion. Widely suggested values [12], [15] of 0.7 for the discharge coefficient are used in the current paper. It should be noted that the Bernoulli's theorem is not strictly applicable since the flows are not dissipationless.

At some horizontal level, between the interface and the ceiling, the hydrostatic pressure will be equal inside and outside the building. This level is known as the 'neutral level', and

is located at a height h_n above the floor. The pressure at the neutral level is denoted as the reference pressure P_o . The location of the neutral level is marked with a dashed line in Figure 1. The hydrostatic pressure at the lower vent inside the compartment is related to the reference pressure as $P_o + \rho gh_n$ and the pressure outside the compartment at the lower vent level is $P_o + \rho_o gh_n$. Since the compartment is well mixed, the pressure drop ΔP_1 across the lower vent is related to the reduced weight of the fluid inside the compartment acting over the distance h_n .

$$\Delta P_1 = \Delta \rho gh_n, \quad (3)$$

where, $\Delta \rho = \rho_o - \rho$, and ρ_o is the density of the ambient air, while ρ is the instantaneous density of the gas mixture in the compartment. Using (3) in (1) we obtain a relationship for velocity v_1 through Vent 1

$$v_1 = \sqrt{2 \frac{\Delta \rho g}{\rho_o} h_n} = \sqrt{2g' h_n}, \quad (4)$$

where $g' = \frac{\Delta \rho g}{\rho_o}$, is the reduced gravity of the fluid. A similar expression can be obtained for the velocity v_3 through the upper vent

$$v_3 = \sqrt{2 \frac{\Delta \rho g}{\rho} (H - h_n)} = \sqrt{2g'(H - h_n)}. \quad (5)$$

For any hydrogen accidental release scenario, it is critical to develop a capability to predict the density of the compartment as a function of time. Since the velocity and volumetric flow rates through the vents are related to the location of the neutral layer, the hydrogen concentration in the compartment is dependent on the instantaneous location of the neutral layer. The rate of accumulation of hydrogen in the compartment is dependent on the rate at which hydrogen gas is released in the compartment and the outflow of hydrogen through the upper vent.

$$V \frac{d(\rho Y_{H_2})}{dt} = \dot{M}_{H_2} - Y_{H_2} * \rho * (a_3 v_3 C_3) \quad (6)$$

where, Y_{H_2} is the instantaneous mass fraction of hydrogen. This ordinary differential equation can be solved to obtain the instantaneous density of hydrogen in the compartment and this in turn can be used to compute the mass fraction or volume fraction of hydrogen and the instantaneous density ρ as a function of time.

An additional equation is needed to predict the location of the neutral layer h_n , needed to obtain the velocity v_3 in Equation (6). Since the volume of the compartment is fixed and assuming that the flow is incompressible, the volumetric flow rate into the compartment must equal the volume of gases leaving the compartment through the upper vent,

$$\dot{V}_{H_2} + a_1 v_1 c_1 = a_3 v_3 c_3 \quad (7)$$

where \dot{V}_{H_2} is the volumetric flow rate (release rate) of hydrogen and is obtained by dividing the mass flow rate of hydrogen \dot{M}_{H_2} by the density of pure hydrogen gas.

Equation (7) along with Equations (6), (4) and (5) form a system of non-linear equations that were solved to obtain the height of the neutral layer h_n , the species density ρY_{H_2} in the compartment and the velocities v_1 and v_3 through the lower and upper vent as a function of time. Equation (6) is an ordinary differential equation that was advanced in time using a second order Runge Kutta (RK) method (midpoint method), followed by a Newton Raphson iteration to solve the volume conservation Equation (7) to obtain the height of the neutral layer and hydrogen species density (hydrogen volume fraction). The volumetric flow rates through the lower and upper vent can be subsequently obtained using Equation (2) along with Equations (4) and (5).

2.1 Justification of the well mixed assumption

The simple analytical model discussed in section 2 was compared with results of a numerical simulation performed using the NIST Fire Dynamics Simulator (FDS). FDS is a CFD package [22] that has been used traditionally by the fire protection community to simulate fires in large buildings and for forensic analysis, and can be used effectively for modeling hydrogen release and dispersion in a compartment. The FDS software has been validated with a series of experiments that have been performed at NIST in which helium was released into a 1/4-scale two-car residential garage [8], [9]. Time resolved measurements of helium volume fractions were made at multiple heights [21] in the model garage during the release and dispersion phase. FDS simulations of the experimental setup were conducted to accurately resolve the entrainment into the buoyant plume and the leakage through the vents. Simulations results indicated that FDS software can be reliably used to predict the hydrogen release and

dispersion in a compartment with specified vent locations. We now discuss that the results of the analytical model discussed in the previous section and the comparison of these results with the simulations from a detailed CFD calculation.

The dimensions of the compartment used for this comparative study were $6.0\text{ m} \times 6.0\text{ m} \times 3.0\text{ m}$, with a total volume of 108 m^3 . Pure hydrogen gas was released through a square release chamber with a cross-section of $0.28\text{ m} \times 0.28\text{ m}$ (cross-section area of 0.0784 m^2). The mass flux of hydrogen gas was set at $0.0177\text{ kg/m}^2/\text{s}$. In the numerical simulations, hydrogen gas was released under a rectangular obstruction ($2.2\text{ m} \times 5.0\text{ m}$), centered over the release chamber and placed at a height of 0.4 m above the floor. The presence of the obstruction results in turbulent mixing between the buoyant hydrogen and the surrounding air. The compartment was vented through two square vents (leaks) located at the top and bottom of the side walls as shown schematically in Figure 1. Each vent had a cross-sectional area of 0.01 m^2 . The computational domain was divided into eight meshes that were chosen to resolve the flow through the release chamber and the vents. Typical fine grid resolution was of the order of 2 cm in the plume region of the flow field. The release period was assumed to last for four hours followed by a four hour dispersion phase. Typical computational costs of a simulation performed on an eight processor machine were approximately 200 hr . Figure 2 shows the numerically predicted hydrogen volume fraction at seven different heights in the compartment. Simulation results indicate that the buoyant plume mixes rapidly with the surrounding air, resulting in an almost uniform mixture of hydrogen and air. The hydrogen volume fraction increases steadily with time until a steady-state is reached at approximately 6000 s . The analytical model developed in the previous section (Figure 2 solid line) compares favorably with the results of the numerical simulations. The steady-state value is also predicted accurately to within 2% of the computed value.

2.2 Effect of Model Parameters

We now study the effect of various parameters in the analytical model on the temporally evolving hydrogen volume fraction and location of the neutral layer in the compartment as well as the time required to reach a steady state.

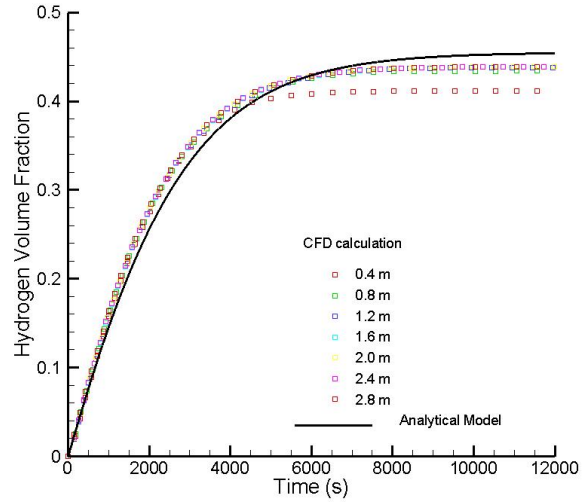


Figure 2: Comparison of numerically predicted hydrogen volume fraction at various heights (symbols) with analytical solution (solid line) for hydrogen release in the partially enclosed compartment.

2.2.1 Effect of hydrogen release rate

Figure 3 shows the effect of changing the hydrogen mass flow rate (release rate) from 5.0 kg/hr to 0.01 kg/hr on the steady-state hydrogen volume fraction and the steady-state height of the neutral layer. The steady-state values were obtained by extending the time dependent calculations until there were no changes in the predicted values. Results from the theoretical model indicate that as the flow rates of hydrogen increase, the hydrogen volume fraction in the compartment increases (decrease in the overall density) and the height of the neutral layer reduces. Figure 4 (left sub-figure) shows the time dependent location of the neutral layer for various hydrogen release rates. For a given vent configuration, the neutral layer stabilizes at a specific height depending on the hydrogen flow rates. As the flow rate increases, the steady-state location of the neutral layer decreases. Results also indicate that the time required to reach a steady-state increases as the hydrogen release rate increases. The volumetric flow rates through the upper and lower vent as a function of time are shown in Figure 4 (right sub-figure) for three different hydrogen release rates. The flow rate through

the lower vent (inflow) is shown as a positive number, while the flow through the upper vent (outflow) is shown as a negative number. The steady-state values of the volumetric flow rates through the upper and lower vent increase as the mass flow rates of hydrogen increase. This can be obtained from Equation (6) which shows that the steady-state volumetric flux is inversely proportional to the hydrogen volume fraction in the compartment.

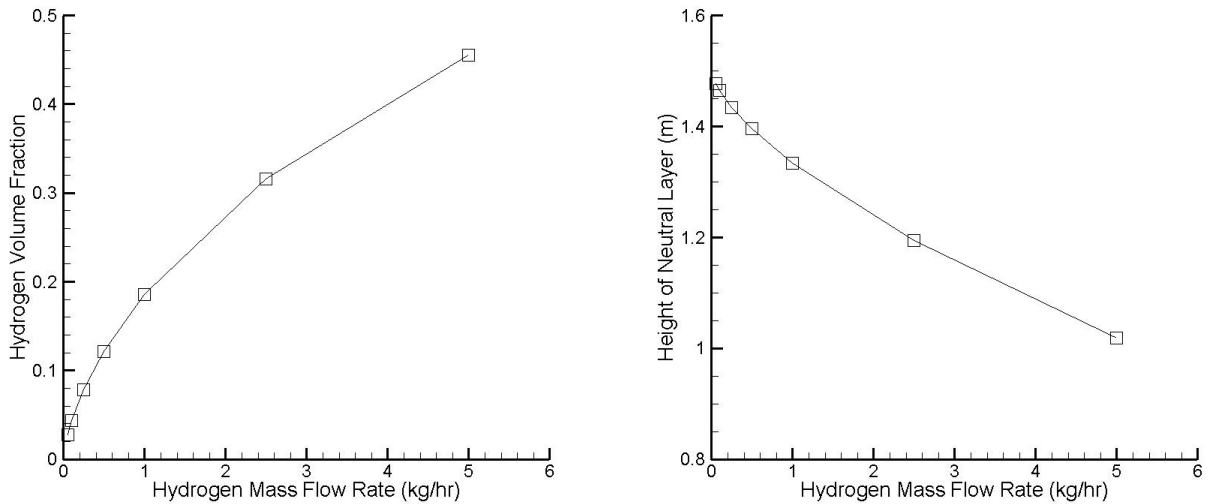


Figure 3: Effect of hydrogen release rate on steady-state hydrogen volume fraction and height of the neutral layer.

2.2.2 Effect of vent cross-sectional area

This sub-section deals with the impact of changing the vent cross-sectional area of both the lower and upper vents simultaneously and its effect on the flow field. As the vent cross-sectional area increases, the steady-state value of hydrogen volume fraction in the compartment reduces for hydrogen flow rate of 5.0 kg/hr , 0.5 kg/hr and 0.05 kg/hr (Figure 5). Reducing the hydrogen volume fraction results in higher compartment density. The height of the neutral layer increases as the vent cross-sectional area increases. As the hydrogen flow rates become smaller (0.05 kg/hr), the hydrogen volume fraction in the compartment becomes very small, and the neutral layer is located at the mid-height (1.5 m) in the compartment. As the vent cross-sectional area increases, the location of the neutral layer approaches

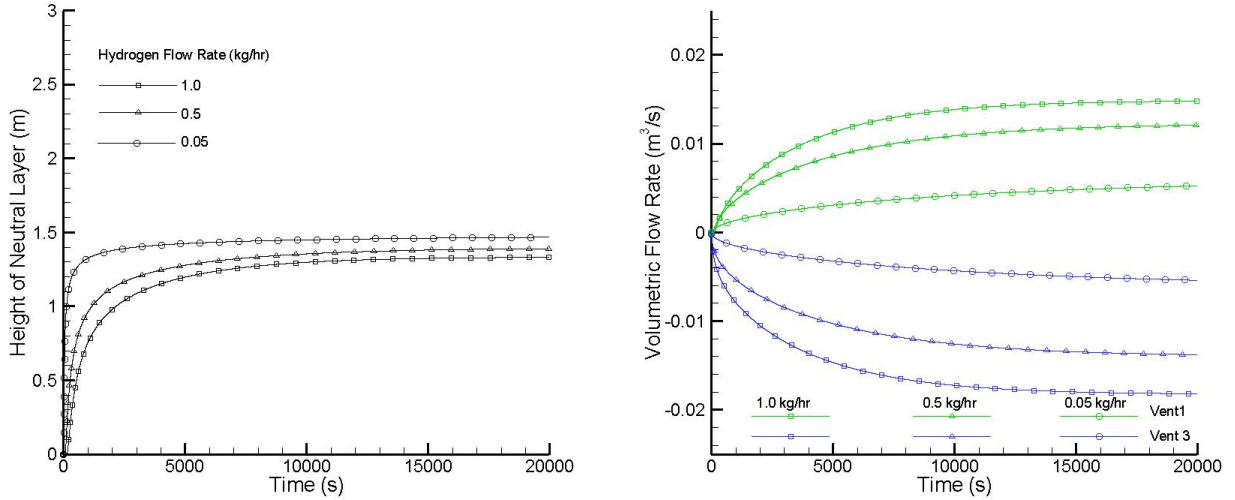


Figure 4: Location of the neutral layer (left sub-figure) and volumetric flow rates (right sub-figure) through the lower vent (inflow) and upper vent (outflow) as a function of time for various hydrogen release rates.

the mid-height of the compartment, since the two vents become equally important in venting the compartment.

2.2.3 Effect of distance between upper and lower vents

Figure 6 shows the effect of changing the distance between the upper and lower vent on the steady-state volumetric flow rates. As the distance between the vents increase, the volumetric flow rates increase. As seen in Equation 5, the volumetric flow rates are proportional to the square root of the distance between the vents. Figure 6 (right sub-figure) shows the transient volumetric flow rates for the upper and lower vents as a function of time, for three different distances between the upper and lower vent. Results shown in Figure 6 also confirm the algebraic relationship expressed in Equation (7). Figure 7 shows that the steady-state value of the hydrogen volume fraction reduces as the distance between the vents increases. This is because the vents are most effective when they are far apart (square root dependence of velocity on distance between the vents) in venting the compartment, which results in smaller value of the hydrogen volume fraction.

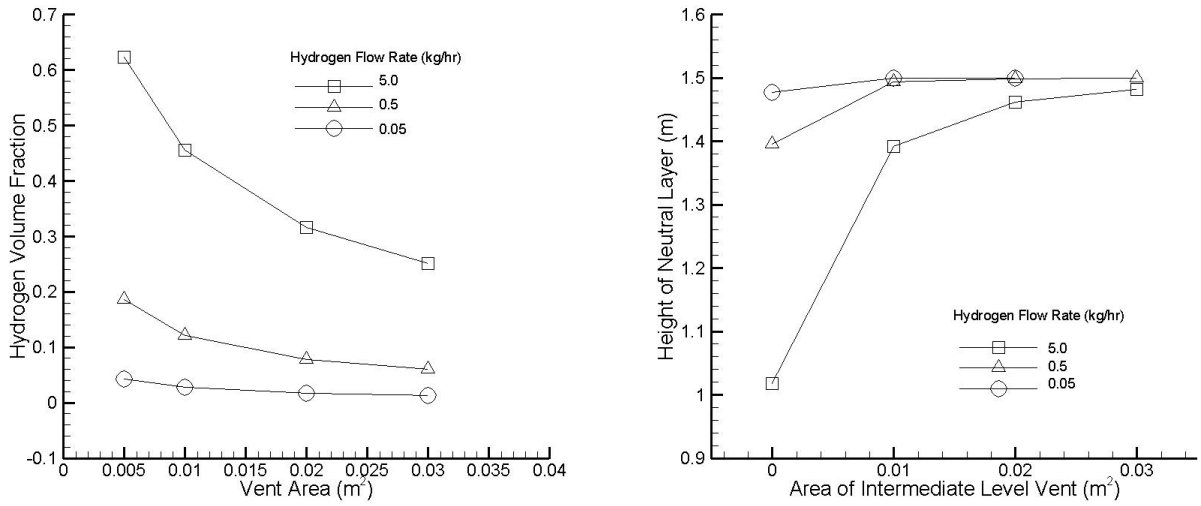


Figure 5: Effect of vent cross-sectional area on steady-state hydrogen volume fraction and height of the neutral layer

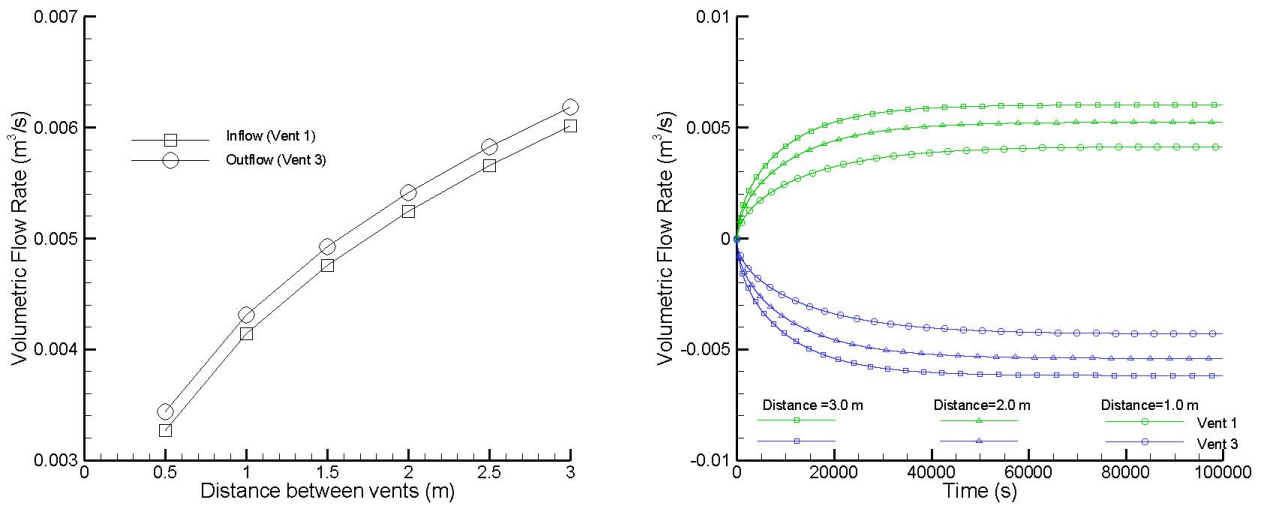


Figure 6: Effect of distance between the two vents on steady-state and transient volumetric flow rate through the upper and lower vent. The hydrogen release rate was set at 0.05 kg/hr.

2.2.4 Effect of using a surrogate gas

Figure 8 shows the effect of using helium as a surrogate gas instead of hydrogen on the volume fraction and height of the neutral layer as a function of time. The volumetric release

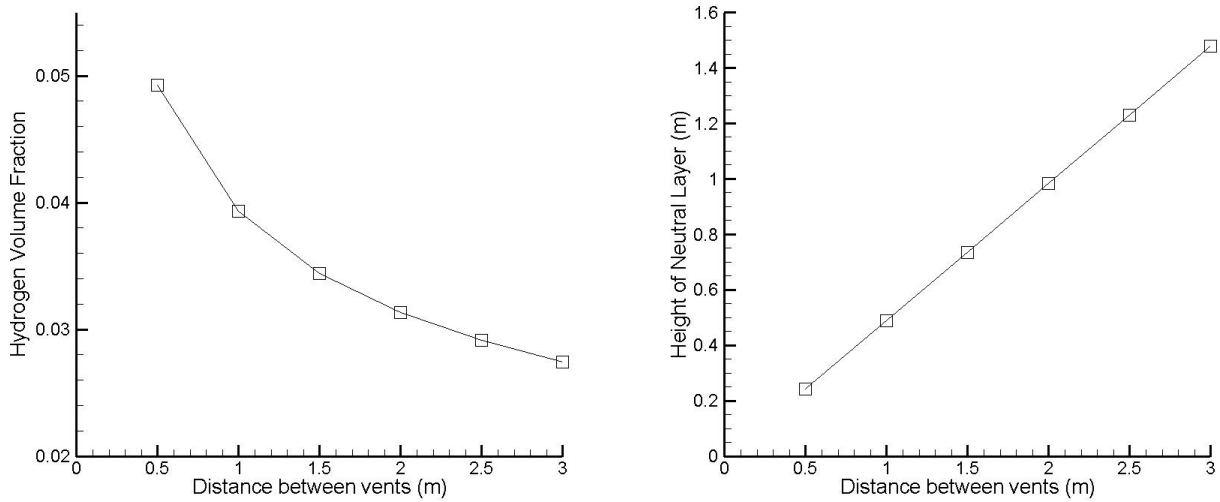


Figure 7: Effect of distance between the two vents on the steady-state values of the volume fraction and height of the neutral layer.

rates of hydrogen and helium were identical to each other ($6.01 \text{ m}^3/\text{hr}$). Note that the mass flow rates were different by a factor of two, due to density differences between hydrogen and helium. Results indicate that the steady-state values of the predicted volume fractions are very close to each other, indicating that use of helium is a good surrogate for hydrogen.

2.2.5 Thermal effects

In this sub-section we demonstrate the application of the theoretical model to study a scenario where there are temperature differences between the outside of the compartment and inside the compartment. Denoting the temperature difference between the exterior and interior of the compartment as ΔT , results in a proportional change in the density of the ambient air. It is assumed that the fresh air that enters the compartment mixes rapidly with the buoyant hydrogen gas and its temperature quickly stabilizes to that inside the compartment. We also assume that there is no heat transfer between the compartment and the cold air outside the compartment. Figure 9 shows the steady-state hydrogen volume fraction and height of the neutral layer as a function of the temperature difference. A negative temperature difference implies that the temperature outside the compartment is less than that inside the compartment. Results indicate that the hydrogen volume fraction under steady-state

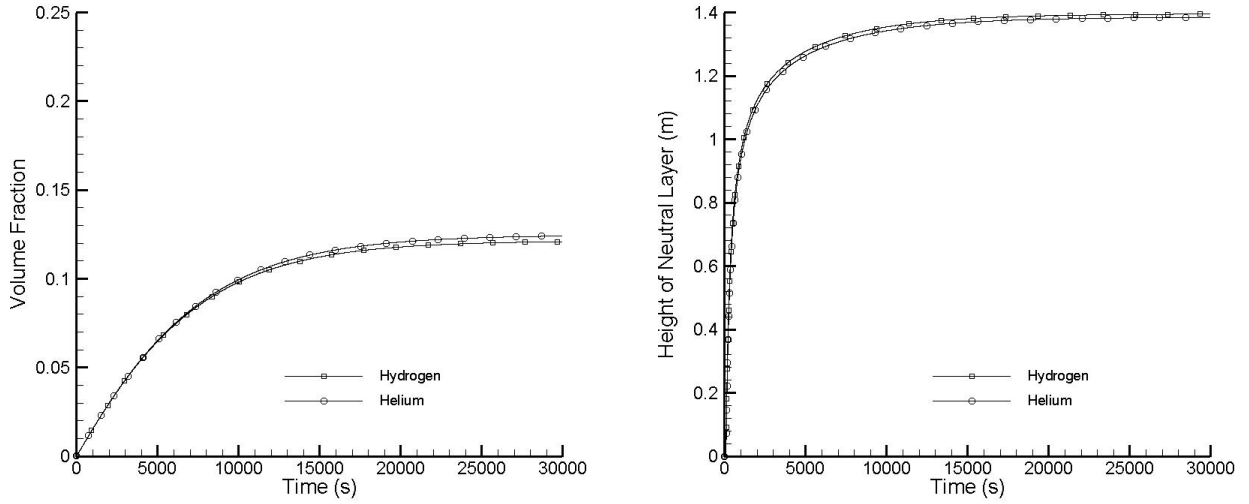


Figure 8: Effect of using a surrogate gas helium as compared to hydrogen on the volume fraction and height of the neutral layer. The volumetric flow rates was held constant for the two cases at $6.01 \text{ m}^3/\text{hr}$.

conditions reduces as the temperature difference between the exterior and interior increases. These results are also consistent with the work reported by Barley et al. [17].

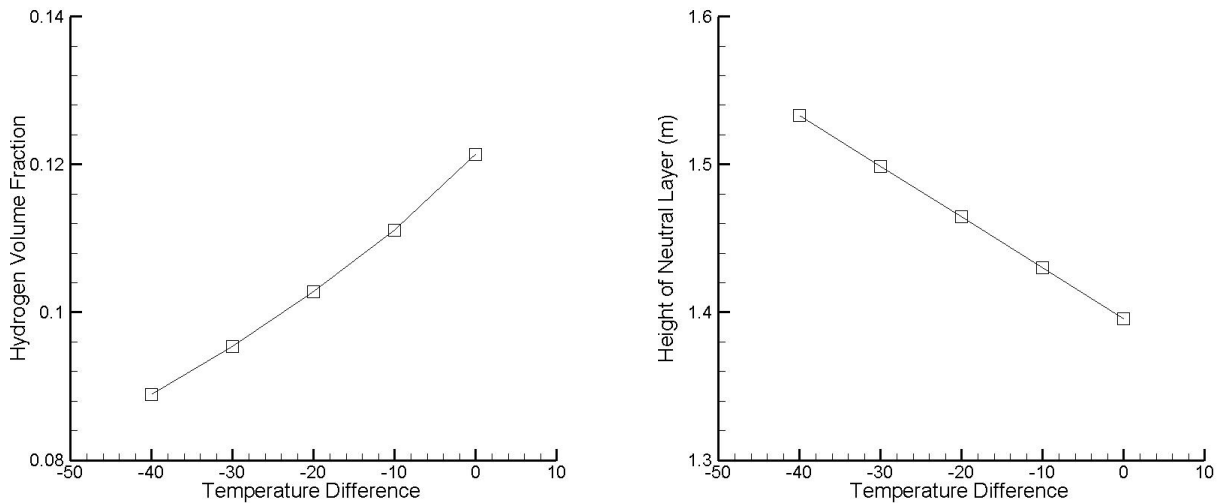


Figure 9: Effect of temperature difference between the outside and inside of the compartment on the steady-state hydrogen volume fraction and height of the neutral layer.

2.3 Effect of additional vents

We now extend the analysis to determine the impact of introducing an intermediate level vent on the density of the compartment and the height of the neutral layer. This intermediate level vent is referred to as "Vent 2" is located at a height h_2 above the floor, and is assumed to have a cross-sectional area of a_2 and a discharge coefficient c_2 . The direction of flow through the intermediate level vent will depend on its location relative to the location of the neutral buoyancy layer. If the middle level vent is located at a height greater than h_n , then the vent will act as an outflow, whereas if it is located at a height less than h_n , it will act as an inflow. This implies that if the vent is located at a height h_n , then no flow will occur through this middle level vent. However, since vents are of finite height and so in the case where the point of neutral buoyancy is contained within the opening, an exchange flow can develop whereby air exits the vent above the point of neutral buoyancy and enters through the lower portion of the vent. We restrict our analysis to the case where the vents are of sufficiently shallow vertical extent that they generally act as pure outlets or inlets.

2.3.1 Intermediate vent located above the neutral layer

We first consider the case in which the location of the intermediate level vent is higher than the neutral buoyancy height ($h_2 > h_n$) as shown in Figure 10. In this case the intermediate vent acts as an outlet. The pressure drop across Vent 2 can be related to the reduced gravity of the interior fluid acting over the distance $h_2 - h_n$. Following the approach discussed in Section 2, we can express the velocity of fluid v_2 exiting from Vent 2 as

$$v_2 = \sqrt{2g'(h_2 - h_n)} \quad (8)$$

Since Vent 2 is an outlet vent, Equation (6) and (7) have to be modified to account for the flow through the intermediate vent, as follows

$$V \frac{d\rho Y_{H_2}}{dt} = \dot{M}_{H_2} - Y_{H_2} * \rho * (a_2 v_2 c_2 + a_3 v_3 c_3) \quad (9)$$

$$\dot{V}_{H_2} + a_1 v_1 c_1 = a_2 v_2 c_2 + a_3 v_3 c_3. \quad (10)$$

Figure 11 shows the effect of introducing an intermediate level vent at a height above the neutral layer. Results shows the steady-state value of the hydrogen volume fraction and

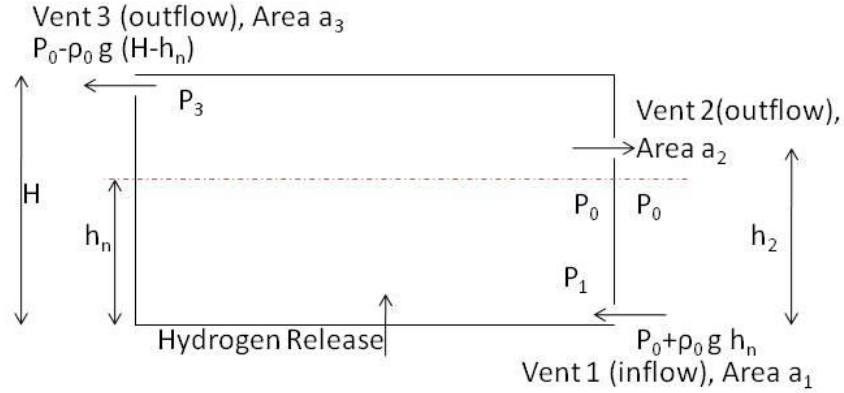


Figure 10: Schematic of a compartment with an intermediate level vent located at a height above the neutral layer.

the height of the neutral layer as a function of the cross-sectional area of the intermediate level vent. The intermediate level vent was located at a height of 1.5 m above the floor. As the area of the intermediate vent increases, the hydrogen volume fraction reduces for all hydrogen release rates. Introduction of the intermediate level vent above the neutral layer raises the neutral buoyancy height. As the size of the intermediate level vent increases such that $a_2 \gg a_1, a_3$, the neutral buoyancy height h_n approaches the height of Vent 2 ($h_n \rightarrow h_2$).

2.3.2 Intermediate vent located below the neutral layer

We now consider the case in which the intermediate level vent is lower than the neutral buoyancy height (Figure 12). In this scenario, a plume of air which descends from the intermediate level vent towards the base. The plume will then spread over the base of the compartment and become mixed by the convection associated with the release of hydrogen. In this case the intermediate level vent acts as an inlet and we again assume that the compartment is well mixed and that the pressure varies hydrostatically with depth.

For Vent 2 to act an inlet, the vent must be below the height of neutral buoyancy (Figure 12). The pressure drop across Vent 2 can be related to the reduced gravity of the interior fluid acting over the distance $h_n - h_2$. As in the previous sub-section, the velocity of the

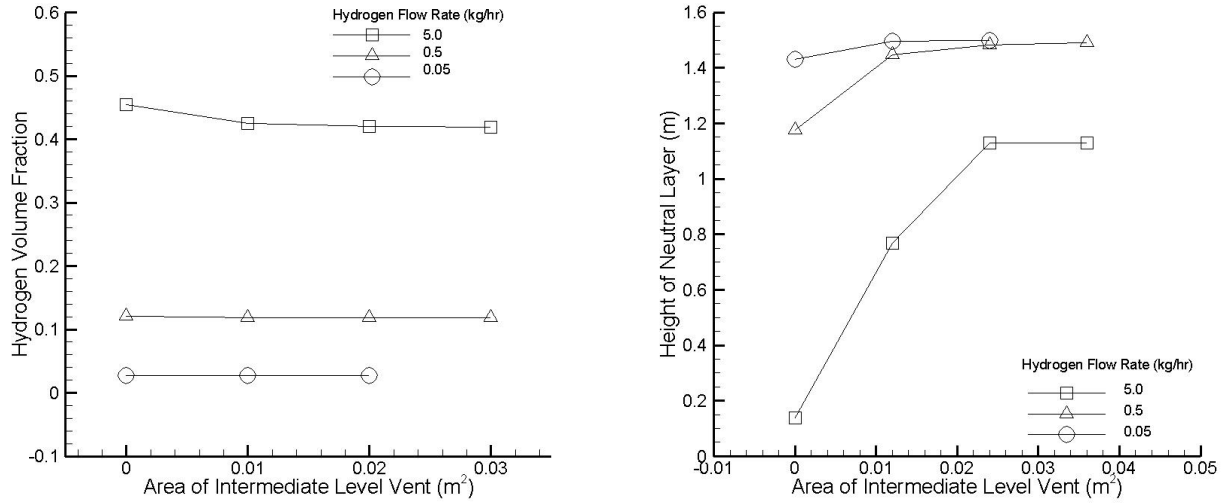


Figure 11: Effect of area of the intermediate level vent on steady-state hydrogen volume fraction and height of the neutral layer.

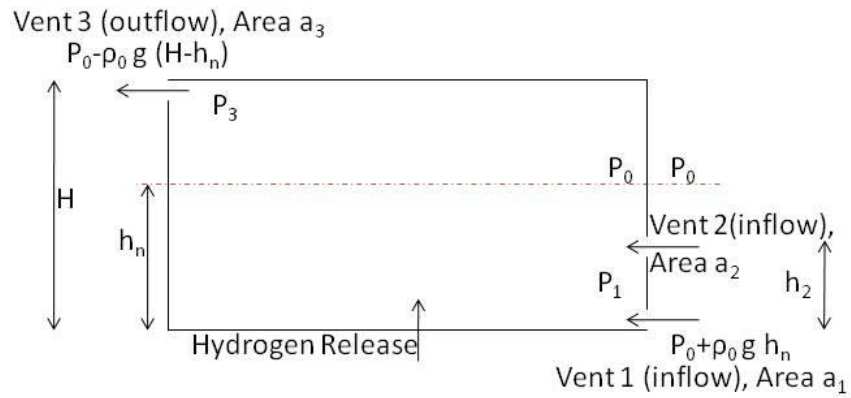


Figure 12: Schematic of a compartment with an intermediate level vent located below the height of the neutral layer.

fluid entering through Vent 2 can be expressed as

$$v_2 = \sqrt{2g'(h_n - h_2)} \quad (11)$$

The mass conservation Equation (6) does not have to be modified, since "Vent 2" is an inlet vent. However, volume conservation for this scenario implies that

$$\dot{V}_{H_2} + a_1 v_1 c_1 + a_2 v_2 c_2 = a_3 v_3 c_3 \quad (12)$$

Introducing an intermediate level vent at a height below the neutral layer also results in a decrease in the steady-state values of the hydrogen volume fraction. As the area of the intermediate vent increases, the hydrogen volume fraction reduces for all hydrogen release rates. Introduction of the intermediate level vent below the neutral layer lowers the neutral buoyancy height. As the size of the intermediate vent increases such that $a_2 \gg a_1, a_3$, the neutral buoyancy height h_n approaches the height of Vent 2 ($h_n \rightarrow h_2$).

Figure 13 shows the effect of the location of the middle vent on hydrogen volume fraction and height of the neutral layer. Results indicate that while the hydrogen volume fraction is relatively insensitive to the location of the middle vent, the height of neutral layer increase with height h_2 of the middle vent. When the intermediate level vent is located at the height of the neutral layer, then the presence of the intermediate level vent has no effect on the volumetric flow rates. However as the intermediate level vent is moved away from the neutral buoyancy height, the total volume flux rises as the area of the additional vent is increased. The additional vent has a greater impact on the total ventilation flow, and hence the hydrogen volume fraction in the compartment, when it is located furthest from the height of the neutral layer.

If the size of the upper vent is different from that of the lower vent, then the flow through the middle vent is still dependent on its location relative to the location of the neutral layer. In the case where the upper vent is much larger than the lower vent, most of the pressure loss through the compartment occurs across the lower vent so that the neutral pressure height is closer to the upper vent ($h_n \rightarrow H$). Similarly when the lower vent is much larger than the upper vent, most of the pressure loss through the compartment occurs across the lower vent and the neutral pressure height approaches the location of the lower vent.

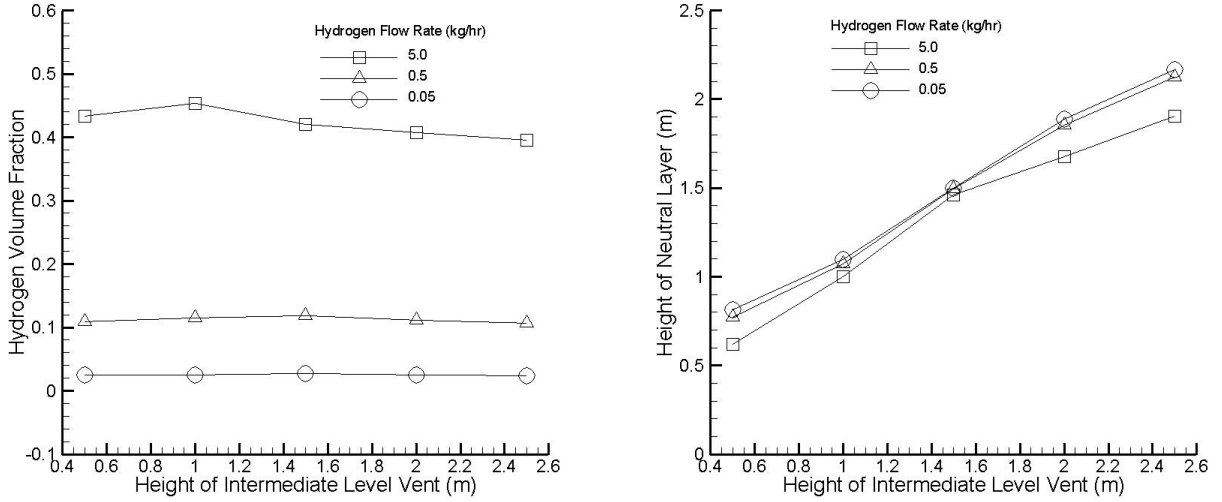


Figure 13: Effect of location of the intermediate level vent on steady-state hydrogen volume fraction and height of the neutral layer.

2.4 Effect of wind on the ventilation of a compartment

If in addition to the buoyancy force that drives the fluid through the vents, there is a steady external wind, then the fluid inside the compartment will be subjected to a force associated with the pressure drop ΔP_w between the windward and leeward openings. In the case where the windward opening is at low-level and the leeward opening is at high-level, the wind adds to the buoyancy driven flow. As a result there is an increased inflow through the lower vent and increased outflow through the upper vent. On the other hand, if the windward opening is the upper vent and the leeward opening is the lower vent, then the wind opposes the buoyancy driven flow. In such a scenario the flow through the vents can be reduced and even change direction depending on the strength of the wind. In this paper we only focus on the wind assisted buoyancy driven flows (Figure 14) and study its effect on hydrogen concentration in a compartment.

It is assumed, as in the previous section, that the heavier fluid flowing through the lower vent gets fully mixed with the buoyant hydrogen gas released in the center of the compartment, due to the presence of the various obstructions. It is also assumed that the variation in pressure within the enclosure is hydrostatic, and that there is a height h_n in the

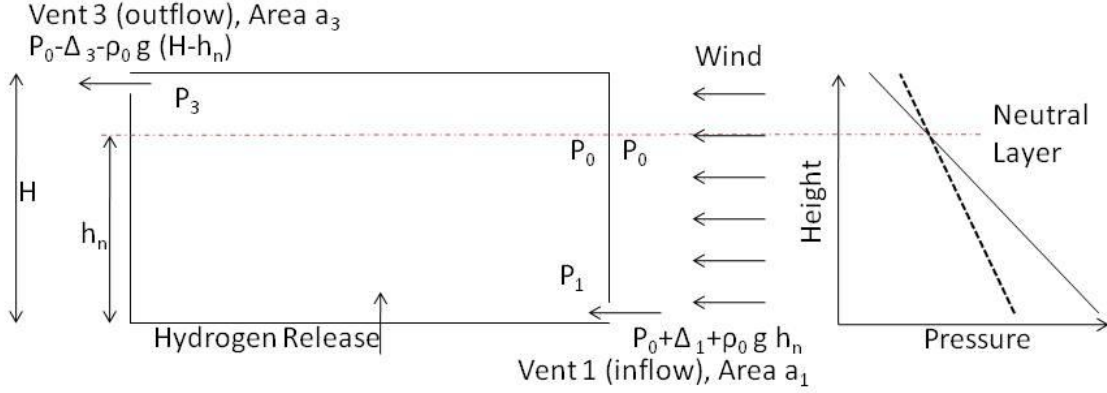


Figure 14: Schematic of a compartment with vents at the top and bottom subjected to a wind that assists the buoyancy driven flow in the compartment.

compartment where the pressure inside and outside the compartment are equal to a reference pressure P_o . If the fluid pressure inside the compartment at height of the lower and upper vent are denoted by P_1 and P_3 , then these pressure can be related to the reference pressure P_o . Thus

$$\begin{aligned} P_1 &= P_o + \rho g h_n \\ P_3 &= P_o - \rho g (H - h_n) \end{aligned} \quad (13)$$

The pressure on the windward opening on the outside of the compartment is higher than the reference pressure P_o by an amount Δ_1 , in addition to the buoyancy pressure. The pressure on the windward opening on the outside of the compartment can be expressed as $P_o + \Delta_1 + \rho_0 g h_n$. Similarly the pressure on the leeward side of the compartment is lower than the reference pressure by an amount Δ_3 . If Δ is the total pressure drop between the windward and leeward openings, then the pressures Δ_1 and Δ_3 can be related to the total pressure drop Δ using

$$\Delta_1 = \frac{h_n}{H} \Delta \quad (14)$$

$$\Delta_3 = \frac{H - h_n}{H} \Delta \quad (15)$$

$$\Delta = \Delta_1 + \Delta_3 \quad (16)$$

Using Bernoulli's theorem, we can derive the velocities through the upper and lower vent as

$$\begin{aligned} v_1 &= \sqrt{2g'h_n + 2 * \Delta_1/\rho_o} \\ v_3 &= \sqrt{2g'(H - h_n) + 2 * \Delta_3/\rho} \end{aligned} \quad (17)$$

The effect of a wind that assists a buoyancy driven flow through a compartment with two vents can be studied by substituting Equation (17) in Equations (6) and (7). The approach for solving these equations is identical to the one discussed in section 2.

Figure 15 shows the effect of increasing the pressure drop Δ due to the wind on the steady-state hydrogen volume fraction and height of the neutral layer. As expected, results indicate that a buoyancy assisted wind flow results in lower hydrogen volume fraction as the pressure drop increases. We also find that the height of the neutral layer increases with the pressure drop.

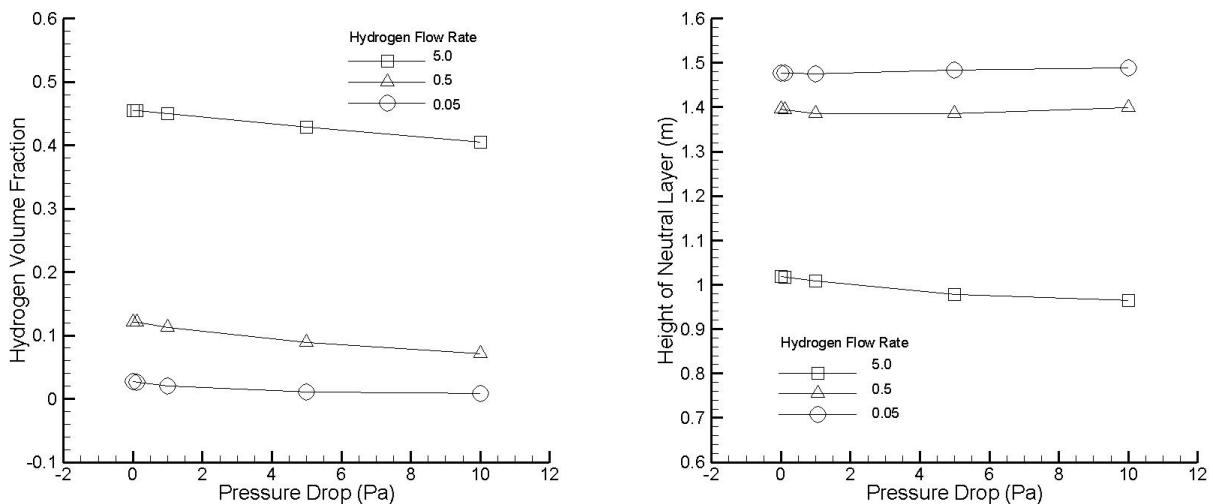


Figure 15: Effect of pressure drop (Δ) due to an assisting wind on steady-state hydrogen volume fraction and height of the neutral layer in a compartment.

2.5 Time required to empty a compartment

The discussion so far has been focused on mixing flows where fresh air driven by buoyancy or an assisting wind, mixes rapidly with the hydrogen released in the compartment, resulting

in a fully mixed flow field. An important problem in hydrogen safety is to understand how a compartment that is initially filled with hydrogen of uniform density would empty through vent with and without the effect of an external wind. Safe use of hydrogen requires one to have a good understanding of how quickly hydrogen can be removed from a partially enclosed space.

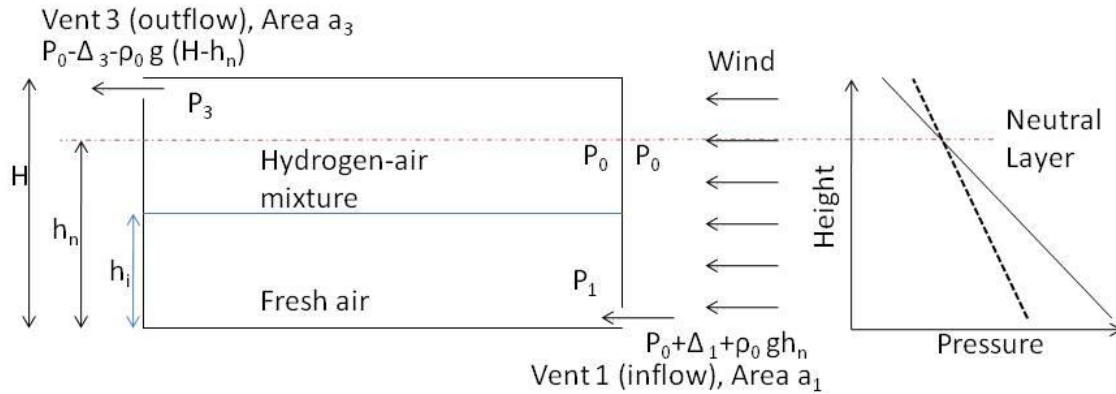


Figure 16: a) Schematic of a compartment with vents at the top and bottom b) The variation of pressure as a function of height within the compartment (dashed line) and outside of the compartment (solid line).

We consider a scenario where a compartment (shown schematically in Figure 16) is initially filled with hydrogen gas of uniform density and we want to predict how the hydrogen gas would empty from a compartment that has two openings (vents), one close to the floor and the other close to the ceiling. The vent configuration is similar to that discussed in Section 2. The flow of hydrogen is assumed to have stopped, either due to a sensor activation that cuts off the hydrogen gas supply, or due to the emptying of the hydrogen tank in the automobile (which has a limited capacity). Under such a scenario, fresh air continues to enter the enclosure through the lower vent (either due to buoyancy driven flow or due to an assisting wind flow). It is further assumed that the incoming fluid does not mix with the fluid in the compartment, but instead forms a layer of increasing depth on the floor of the compartment. This is primarily due to the fact that the hydrogen flow has been discontinued and there is no longer any mixing of the hydrogen with the air. The location of this interface

between the fresh incoming fluid and hydrogen-air mixture is referred to by a height h_i , which is a function of time. Initially the interface height is zero ($h_i = 0$) indicating a fully mixed fluid in the compartment. The compartment will be considered to be empty when the interface height is equal to the height of the compartment ($h_i = H$). We also assume that the horizontal area of the compartment is much larger than the cross-sectional area of either openings, so that the velocity of the interface that exists between the fresh air and the less dense hydrogen air mixture is negligible.

Figure 16 shows a schematic diagram of the location of the interface height relative to the location of the neutral layer in a compartment with two vents and subjected to an assisting wind similar to that described in section 2.4. Again assuming that the pressure varies within the enclosure is hydrostatic, the fluid pressure inside the enclosure at the height of the lower vent (P_1) and the upper vent (P_3), can be written as

$$P_1 = P_o + \rho g(h_n - h_i) + \rho_o g h_i \quad (18)$$

$$P_3 = P_o - \rho g(H - h_n) \quad (19)$$

The pressure on the windward and leeward opening on the outside of the compartment can be related to the reference pressure P_o are identical to those used in Section 2.4 and shown in the schematically in Figure 16.

Using Bernoulli's theorem, we can derive the velocities through the upper and lower vent as

$$v_1 = \sqrt{2g'(h_n - h_i) + 2 * \Delta_1 / \rho_o} \quad (20)$$

$$v_3 = \sqrt{2g'(H - h_n) + 2 * \Delta_3 / \rho}$$

where Δ_1 and Δ_3 are related to the pressure drop between the windward and leeward openings Δ and shown in Equation (14). In addition, the flux that enters the compartment equals the flux that leaves the compartment,

$$Q = a_1 v_1 c_1 = a_3 v_3 c_3 \quad (21)$$

Also the rate at which the light fluid in the compartment is replaced by dense fluid, or the rate at which the location of the interface between the light fluid and fresh air increases can

be expressed as an ordinary differential equation

$$\frac{dh_i}{dt} = \frac{Q}{S}, \quad (22)$$

where S is the horizontal cross-sectional area of the compartment. Equation (22) is solved by a second order accurate RK method subject to the initial condition that the interface height is zero initially, to obtain the instantaneous height of the interface. This is followed by a Newton Raphson iterative solution to obtain the location of the neutral layer. It should be noted that the density of the fluid above the interface does not change as it leaves the compartment. The location of the interface and the height of the neutral layer evolve with time and the compartment is completely empty when $h_i \rightarrow H$.

Figure 17 shows the results of emptying a compartment with and without an assisting wind flow. The left sub-figure in Figure 17 shows the effect of initial compartment density with no prevailing wind on the time to empty the compartment. Emptying of the compartment when there is no wind can be studied by setting the overpressure to zero in Equations (21). Results indicate that the emptying time increases as the compartment density increase or the volume fraction of hydrogen reduces. This is due to the dependence of volumetric flow rates on density difference ($\Delta\rho$), which results in smaller volumetric flow rates and longer times to empty the compartment. The right sub-figure in Figure 17 shows the effect of changing the overpressure due to the wind on emptying time. For each hydrogen flow rate, results indicate that the time to empty the compartment reduces as the wind overpressure increases. This implies that the fastest way to reduce the hydrogen volume fraction is to blow on the vents.

Figure 18 shows the location of the neutral layer and height of the interface between fresh air and the lighter hydrogen air mixture as a function of time during the emptying of the compartment. During this phase, the dense air coming in through the lower vent displaces the lighter fluid and pushes it out of the upper vent. As the location of the interface changes with time, the height of the neutral layer also adjusts. The results are shown as a function of the initial hydrogen flow rates varying from 5.0 kg/hr to 0.05 kg/hr. Results indicate that the initial location of the neutral layer is at the mid-height of the compartment for all initial hydrogen release rates. As the hydrogen-air mixture is displaced, the height of the interface

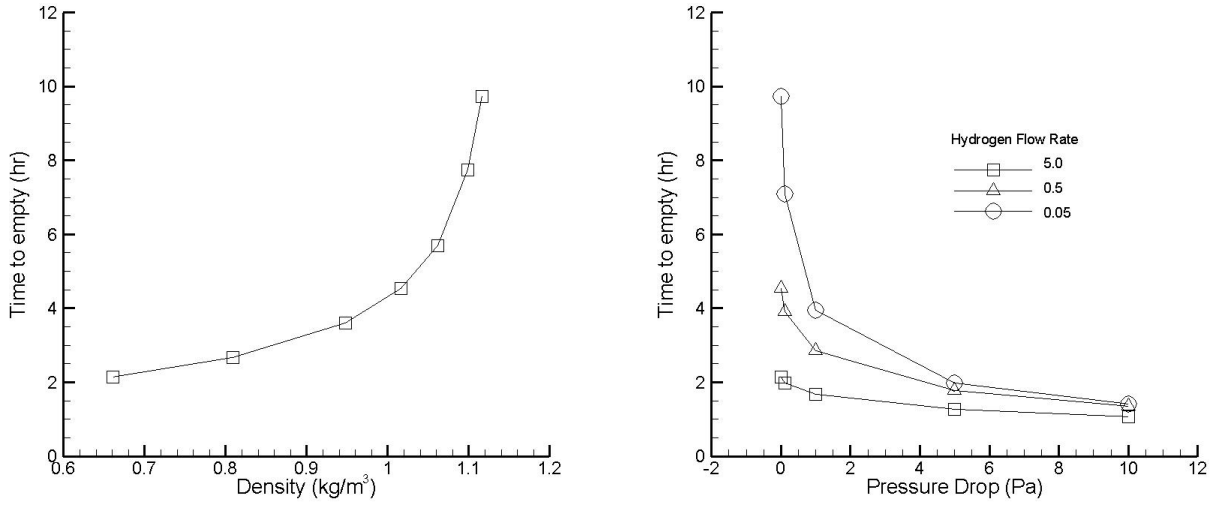


Figure 17: Time required to empty a compartment with an assisting wind flow (right sub-figure) plotted as a function of the pressure drop for various initial values of hydrogen release rates. The time required to empty a compartment in the absence of any wind as a function of initial compartment density is shown in the left sub-figure.

increases with time until the interface is located at the top of the compartment.

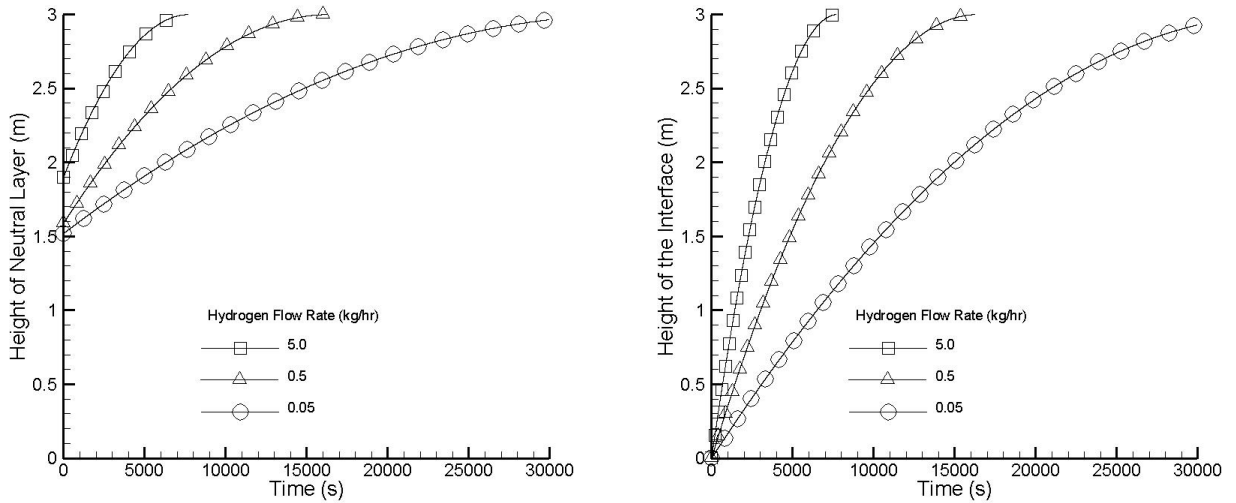


Figure 18: Location of the neutral layer and height of the interface as a function of time during the empty phase for various initial hydrogen release rates

Figure 19 shows the height of the neutral layer as a function of time during the release phase (mixing phase) as well as the emptying phase (displacement phase) for hydrogen release rate of 5.0 kg/hr (left sub-figure) and 0.05 kg/hr (right sub-figure). The release phase last for first forty hours and was chosen to be large enough so as to establish a steady-state for all initial hydrogen flow rates. Results indicate that during the release phase the height of the neutral layer quickly adjusts to its steady-state level. When the hydrogen release is terminated, the height of the neutral layer adjusts abruptly to the mid height of the compartment. This is followed by a rapid increase in the location of the neutral layer during the emptying phase. The volumetric flow rates during the release phase and emptying phase for hydrogen release rate of 5.0 *kg/hr* and 0.05 *kg/hr* is shown in Figure 20. The steady-state volumetric flow rate during the release phase are higher when the hydrogen release rate is higher. During the emptying phase, the drop in the volumetric flow rates is steeper for higher hydrogen release rates. This is due to the relative location of the neutral layer in the two cases and its effect on ventilation through the upper and lower vent. These results indicate that the analytical model is capable of capturing the important physical process observed during the release phase as well as the emptying phase.

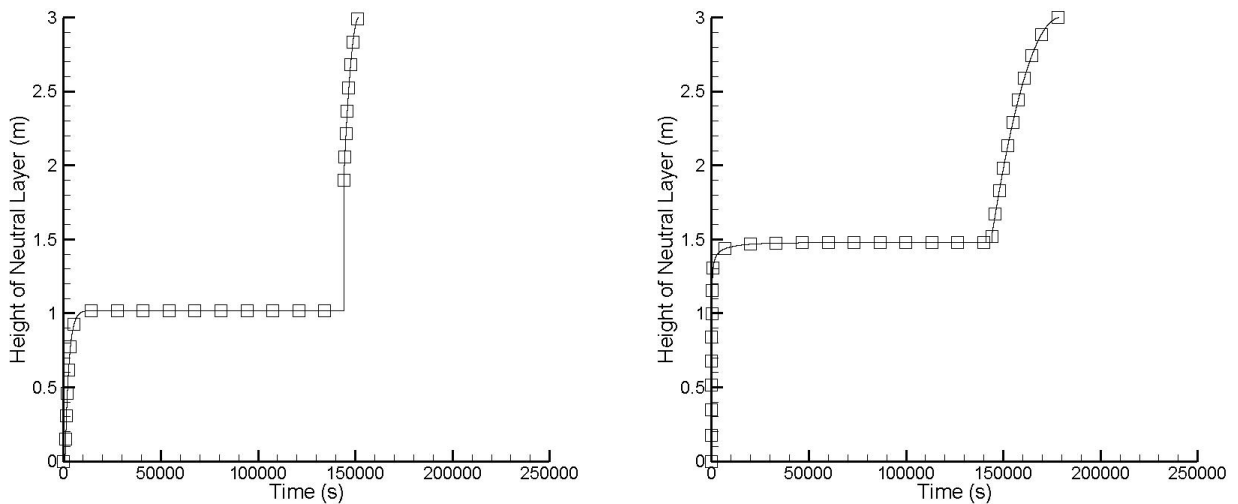


Figure 19: Height of the neutral layer as a function of time during the release phase (mixing phase) as well as the emptying phase (displacement phase) for hydrogen release rate of 5.0 *kg/hr* (left) and 0.05 *kg/hr* (right).

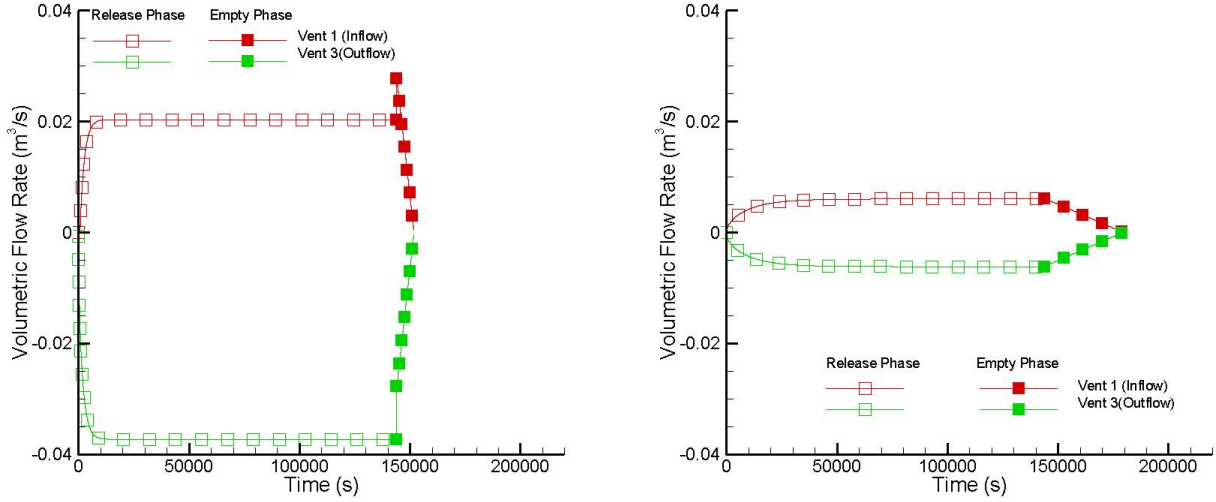


Figure 20: Volumetric flow rates through the upper and lower vent during the release phase (mixing phase) as well as the emptying phase (displacement phase) for hydrogen release rate of 5.0 kg/hr (left) and 0.05 kg/hr (right).

3 Conclusions and Discussion

A simple theoretical model has been presented for understanding the natural and forced (wind aided) mixing and dispersion of hydrogen in partially confined spaces with vents at multiple levels to support the development of appropriate hydrogen safety codes and standards. The transient analysis involves the determination of the position of the neutral buoyancy layer, where the pressure in the compartment is equal to that of the exterior. The effect of hydrogen release rates, vent location and cross-sectional area as well as thermal effect on hydrogen volume fraction in the compartment is presented. Steady state hydrogen volume fraction in the compartment is lower when the hydrogen release rate is smaller and the vent cross-sectional area is larger. Results indicate that natural ventilation of the compartment is most efficient when the vents are located far away from the location of the neutral plane. The steady state hydrogen volume fraction in the compartment reduces as additional intermediate vents are introduced in the walls and when the vents are located far away from the neutral plane. The role of an external wind that assists the buoyancy driven flow is discussed and simple models are developed to understand how long it takes to empty

a compartment. Results of this study indicate that the fastest way to reduce flammable levels of hydrogen concentration in a compartment is to blow on the vents.

The analysis has been limited to conditions where the hydrogen mixes rapidly with the surrounding air following its release under an obstruction, resulting in a well-mixed condition. Future work will focus on conditions where the hydrogen released does not mix immediately with the surrounding air, but entrains air as the plume rises towards the ceiling. The effect of temperature differences between the compartment and the surroundings has been considered, but the analysis is limited to conditions where there is no heat transfer between the compartment and the surroundings. The effect of pressure differences between the windward and leeward sides of the compartment due to wind that assists the buoyancy driven flow was considered in this paper, but transient effects including the effect of wind generated vortices were not considered. The effect of a wind that opposes the buoyancy induced flow is more complex, since it can change the direction of the flow through the upper and lower vents and can result in conditions where the flow through both the vents is blocked. Future research will extend the analysis to conditions where the wind opposes the buoyancy induced flow and its effect on hydrogen concentration in the compartment.

References

- [1] Hydrogen Technology, Aline Leon, Editor, Springer 2008.
- [2] Proceedings of the 2nd International Conference on Hydrogen Safety, September 2007.
- [3] Proceedings of the 3rd International Conference on Hydrogen Safety, September 2009.
- [4] M. R. Swain, E. S. Grilliot and M. N. Swain, "Advances in Hydrogen Energy," New York, Kluwer Academic Publishers, Plenum Press, Dordrecht, p. 163-173, 2000.
- [5] M. R. Swain, P. Filoso, E. S. Grilliot and M. N. Swain, International Journal of Hydrogen Energy, 28, 229-248, 2003.
- [6] M. R. Swain, J. Shriber, Energy and Fuels, 12, 83-89,1998.
- [7] A. G. Venetsanos, E. Papanikolaou, M. Delichatsios, J. Garcia, O. R. Hansen, M. Heitsh, A. Huser, W. Hahn, T. Jordan, J-M. Lacomme, H. S. Ledin, D. Markarov, P. Middha, E. Studer, A. V. Tchoulvelev, A. Teodorczyk, F. Verbecke, M. M. vander Voort, "An inter-comparison exercise on the capabilities of CFD models to predict the short and long term distribution and mixing of hydrogen in a garage, 2nd International Conference on Hydrogen Safety, 2007.
- [8] K. Prasad, N. Bryner, M. Bundy, T. Cleary, A. Hamins, N. Marsh, W. Pitts, J. Yang, "Numerical Simulation of Hydrogen Leakage and Mixing in Large Confined Spaces," Proceedings of the NHA Annual Hydrogen Conference, 2008.
- [9] K. Prasad, W. Pitts, J. Yang, "A Numerical Study of Hydrogen or Helium Release and Mixing in Partially Confined Space," Proceedings of the NHA Annual Hydrogen Conference, 2009.
- [10] P. F. Linden, G. F. Lane-Serff and D. A. Smeed, "Emptying filling boxes: the fluid mechanics of natural ventilation," J. Fluid Mech, (1990), vol. 212, pp. 309-335.
- [11] N. B. Kaye and G. R. Hunt, "Time-dependent flows in an emptying filling box," J. Fluid Mech. (2004), vol. 520, pp. 135-156.

- [12] B. Lishman and A. W. Woods, "The control of naturally ventilated buildings subject to wind and buoyancy," *J. Fluid Mech.* (2006), vol. 557, pp. 451-471.
- [13] G.K. Batchelor, "An Introduction of Fluid Dynamics," Cambridge University Press, 1967.
- [14] W.D. Baines, J. S. Turner, "Turbulent buoyant convection from a source in a confined region," *J. Fluid Mech.*, 37, 51-80, 1969.
- [15] C. Gladstone, and A. W. Woods. "On Buoyancy-driven natural ventilation of a room with a heated floor," *J. Fluid Mech.* (2001), vol. 441, pp. 293-314.
- [16] J. Zhang, M. Hagen, D. Bakirtzis, M. A. Delichatsios, A. G. Venetsanos, "Numerical Studies of Dispersion and Flammable Volume of Hydrogen in Enclosures," Proceedings of 2nd International Conference on Hydrogen Safety, 2007.
- [17] C. D. Barley, K. Gawlik, J. Ohi and R. Hewett, "Analysis of Buoyancy Driven Ventilation of Hydrogen From Buildings," Proceedings of 2nd International Conference on Hydrogen Safety, 2007.
- [18] A. V. Tchouvelev, J. DeVaal, Z. Cheng, R. Corfu, R. Rozek and C. Lee, "Modeling of Hydrogen Dispersion Experiments for SAE J2578 Test Method Development," Proceedings of the Second International Conference on Hydrogen Safety, 2007.
- [19] Y. Ishimoto, E. Merilo, M. Groethe, S. Chiba, H. Iwabuchi, K. Sakata, "Study of Hydrogen Diffusion and Deflagration in a Closed System", Proceedings of the Second International Conference on Hydrogen Safety, 2007.
- [20] J. M. Lacombe, Y. Dagba, D. Jamois, L. Perrette, Ch. Proust, "Large-Scale Hydrogen Release in an Isothermal Confined Area, Proceedings of the Second International Conference on Hydrogen Safety, 2007.
- [21] W. M. Pitts, K. Prasad, J. C. Yang, M. G. Fernandez, "Experimental Characteristics and Modeling of Helium Dispersion in a 1/4-Scale Two-Car Residential Garage," Proceedings of the Third International Conference on Hydrogen Safety, 2009.

- [22] K. McGrattan, S. Hostikka, J. Floyd, H. Baum, R. Rehm and R. McDermott, "Fire Dynamics Simulator (Version 5) Technical Reference Guide, Special Publication 1018-5, National Institute of Standards and Technology, Gaithersburg, MD, 2007.

List of Figures

1	Schematic diagram of a compartment with vents at the top and bottom showing the location of the neutral layer. The variation of pressure as a function of height within the compartment (dashed line) and outside of the compartment (solid line) are also indicated.	7
2	Comparison of numerically predicted hydrogen volume fraction at various heights (symbols) with analytical solution (solid line) for hydrogen release in the partially enclosed compartment.	11
3	Effect of hydrogen release rate on steady-state hydrogen volume fraction and height of the neutral layer.	12
4	Location of the neutral layer (left sub-figure) and volumetric flow rates (right sub-figure) through the lower vent (inflow) and upper vent (outflow) as a function of time for various hydrogen release rates.	13
5	Effect of vent cross-sectional area on steady-state hydrogen volume fraction and height of the neutral layer	14
6	Effect of distance between the two vents on steady-state and transient volumetric flow rate through the upper and lower vent. The hydrogen release rate was set at 0.05 kg/hr	14
7	Effect of distance between the two vents on the steady-state values of the volume fraction and height of the neutral layer.	15
8	Effect of using a surrogate gas helium as compared to hydrogen on the volume fraction and height of the neutral layer. The volumetric flow rates was held constant for the two cases at $6.01 \text{ m}^3/\text{hr}$	16
9	Effect of temperature difference between the outside and inside of the compartment on the steady-state hydrogen volume fraction and height of the neutral layer.	16
10	Schematic of a compartment with an intermediate level vent located at a height above the neutral layer.	18

11	Effect of area of the intermediate level vent on steady-state hydrogen volume fraction and height of the neutral layer.	19
12	Schematic of a compartment with an intermediate level vent located below the height of the neutral layer.	19
13	Effect of location of the intermediate level vent on steady-state hydrogen volume fraction and height of the neutral layer.	21
14	Schematic of a compartment with vents at the top and bottom subjected to a wind that assists the buoyancy driven flow in the compartment.	22
15	Effect of pressure drop (Δ) due to an assisting wind on steady-state hydrogen volume fraction and height of the neutral layer in a compartment.	23
16	a) Schematic of a compartment with vents at the top and bottom b) The variation of pressure as a function of height within the compartment (dashed line) and outside of the compartment (solid line).	24
17	Time required to empty a compartment with an assisting wind flow (right sub-figure) plotted as a function of the pressure drop for various initial values of hydrogen release rates. The time required to empty a compartment in the absence of any wind as a function of initial compartment density is shown in the left sub-figure.	27
18	Location of the neutral layer and height of the interface as a function of time during the empty phase for various initial hydrogen release rates	27
19	Height of the neutral layer as a function of time during the release phase (mixing phase) as well as the emptying phase (displacement phase) for hydrogen release rate of 5.0 <i>kg/hr</i> (left) and 0.05 <i>kg/hr</i> (right).	28
20	Volumetric flow rates through the upper and lower vent during the release phase (mixing phase) as well as the emptying phase (displacement phase) for hydrogen release rate of 5.0 <i>kg/hr</i> (left) and 0.05 <i>kg/hr</i> (right).	29